International Journal of Thermophysics, Vol. 25, No. 5, September 2004 (© 2004)

Nonequilibrium Molecular Dynamics Simulations of Molten Sodium Chloride[1]

J. Petravic[2–4] and J. Delhommelle[5]

The main problems arising in all far-from-equilibrium simulations come from temperature control. When local flows become important, it is not a simple matter to distinguish between the flow velocity and thermal motion. A way to bypass this problem is to control the temperature given by the "configurational expression", which does not depend on velocity. The responses of molten NaCl to strong shear and strong constant and oscillating electric fields using kinetic and configurational thermostats are compared. The differences in response increase with the increase in the external perturbation, and in very strong fields one can observe striking structural differences. In the case of shear flow, the differences are of a general nature seen in all liquids (the appearance of a string phase with kinetic thermostats), while in an electric field they are peculiar to ionic fluids and are related to the degree of dissociation. Some structural properties can be deduced by evaluating the configurational temperature expression.

KEY WORDS: conductivity; molecular dynamics; molten salts; thermostats; viscosity.

1. INTRODUCTION

When a liquid is subjected to an external perturbation without being allowed to interact with an environment, the work done by the field is

[1]Paper presented at the Fifteenth Symposium on Thermophysical Properties, June 22–27, 2003, Boulder, Colorado, U.S.A.

[2]Research School of Chemistry, The Australian National University, Canberra ACT 0200, Australia.

[3]Present Address: School of Chemistry F11, The University of Sydney, NSW 2006, Australia.

[4]To whom correspondence should be addressed. E-mail: janka@chem.usyd.edu.au

[5]Équipe de Chimie et Biochimie Théoriques, UMR 7565, Université Henri Poincaré, BP 239, F-54506 Vandœuvre-lès-Nancy Cedex, France.

0195-928X/04/0900-1375/0

converted into internal energy, which increases indefinitely. This is evidenced in the simultaneous generation of a response flow and an increase of temperature. The characteristics of the flow change as the system heats up passing through states of different equilibrium properties. If the system interacts with the environment, the heat generated by the work of external forces is dissipated through processes of conduction, convection and radiation, and fluxes and thermodynamic quantities reach steady-state values.

The aim of a nonequilibrium molecular dynamics (NEMD) simulation is to investigate the properties of these non-equilibrium steady states in model systems of typically several hundred interacting particles with the appropriate boundary conditions. It is important to incorporate into the particle equations of motion a mechanism that accounts for the heat loss in an averaged way. This is achieved by adding a constraint [1] or a feedback [2] term that controls the value of a microscopic expression for temperature.

In equilibrium, the most commonly used expression is the kinetic temperature definition, defined by the equipartition theorem as proportional to the second moment of velocity fluctuations. This definition is consistent with the Maxwell–Boltzmann equilibrium distribution. Since the distribution function is not known far from equilibrium, this definition is *ad hoc* extended to nonequilibrium steady states. In this case "thermal motion", which defines temperature, is defined with respect to the velocity of local flow. In practice, it is often impossible to determine which part of particle velocity is due to the local flow, and which is due to thermal motion, especially in strong fields generating strong dissipative fluxes [3,4]. In such a situation, controlling different definitions of kinetic temperature can result in systems behaving in a qualitatively different manner [3,4].

Recently, an alternative definition of "configurational" temperature, solely in terms of positions [5,6], has been proposed. In equilibrium, both kinetic and configurational definitions are equivalent and can be derived from the thermodynamic temperature definition as the inverse rate of change of entropy with internal energy at constant volume, using the Gibbs' microscopic expression for entropy [5]. Far from equilibrium, temperature is not a well-defined quantity. Extending both kinetic and configurational definitions to systems out of equilibrium implies the approximation that the phase-space probability distribution stays equal to the equilibrium probability distribution. This approximation is assumed in both types of temperature definitions when used out of equilibrium. However, the configurational expression does not contain the additional error of incorrect estimations of flow velocities and is therefore considered "more correct".

In this work, we compare the response of molten sodium chloride obtained with the control of kinetic and configurational temperature, when it is subjected to two types of external perturbation: shear [7] and electric field [8]. The aim is to determine the flow properties of a molten salt far from equilibrium, and assess the influence of the thermostat type on the result.

The configurational temperature can be vaguely associated with positional disorder related to structural properties, but the expressions for configurational temperature are complex and hard to interpret. Our other aim is to gain further understanding of their physical meaning by calculating them in different systems and under different conditions.

2. MODEL AND SIMULATION DETAILS

We used the Born-Huggins-Mayer potential to describe the pair interactions,

$$\Phi_{ij}(r_{ij}) = z_i z_j \frac{e^2}{r_{ij}} + A_{ij} \exp\left[B\left(\sigma_i + \sigma_j - r_{ij}\right)\right] - \frac{C_{ij}}{r_{ij}^6} - \frac{D_{ij}}{r_{ij}^8}, \tag{1}$$

where z_i and z_j are the formal charges of ions i and j, respectively, and A_{ij}, B, $(\sigma_i + \sigma_j)$, C_{ij}, and D_{ij} are parameters for molten NaCl determined by Tosi and Fumi [9].

Shear flow was simulated using Sllod [10] equations of motion at constant volume. When the kinetic temperature is controlled by the Gauss minimal constraint method, the equations of motion are

$$\begin{aligned} \dot{\mathbf{r}}_i &= \mathbf{p}_i/m_i + \mathbf{e}_x \gamma y_i \\ \dot{\mathbf{p}}_i &= \mathbf{F}_i - \mathbf{e}_x \gamma p_{yi} - \alpha \mathbf{p}_i, \end{aligned} \tag{2}$$

where $\mathbf{r}_i$ ($\mathbf{p}_i$) is the position ("peculiar" momentum) of ion i, $\mathbf{F}_i$ is the total force on ion i from interaction potential Eq. (1), m_i is its mass, and γ is the imposed strain rate. Shear is applied in the x direction, and $\mathbf{e}_x$ is the unit vector along the x-axis. Peculiar momentum is the momentum of a particle relative to the linear "streaming velocity" velocity profile $u_x = \gamma y$, where y is the Cartesian component of position. The thermostat multiplier α, which constrains the peculiar kinetic energy $\Sigma_i \mathbf{p}_i^2/2m_i$ to a constant, is

$$\alpha = \frac{\sum_i \left(\mathbf{F}_i \cdot \mathbf{p}_i - \gamma p_{xi} p_{yi}\right)/m_i}{\sum_i \mathbf{p}_i^2/m_i}. \tag{3}$$

In this case, the conserved temperature T_{KIN} is given by the kinetic definition,

$$\frac{3}{2}Nk_{\mathrm{B}}T_{\mathrm{KIN}} = \left\langle \sum_{i=1}^{N} \frac{p_i^2}{2m_i} \right\rangle, \tag{4}$$

where the triangular brackets denote the ensemble average.

The configurational temperature, defined as [6]

$$k_{\mathrm{B}}T_{\mathrm{CONF}} = \frac{\left\langle \sum_i \mathbf{F}_i^2 \right\rangle}{\left\langle -\sum_i \nabla_i \cdot \mathbf{F}_i \right\rangle}, \tag{5}$$

is controlled using a Nosé–Hoover type integral feedback applied to position equations of motion [11],

$$\begin{aligned} \dot{\mathbf{r}}_i &= \mathbf{p}_i/m_i + \mathbf{e}_x \gamma y_i + \frac{s}{T_0}\frac{\partial T_{\mathrm{CONF}}}{\partial \mathbf{r}_i} \\ \dot{\mathbf{p}}_i &= \mathbf{F}_i - \mathbf{e}_x \gamma p_{yi} \\ \dot{s} &= -Q(T_{\mathrm{CONF}} - T_0)/T_0, \end{aligned} \tag{6}$$

where Q is a damping constant and s is the feedback variable.

A constant electric field E_{EL} or alternating electric field $E_{\mathrm{EL}} = E_0 \cos \omega_0 t$ was applied along the x-axis. In this case the kinetic temperature is defined in terms of motion with respect to the flow velocity $\mathbf{u}_\nu$ of each type of ion ($\nu = +, -$) [12],

$$\mathbf{u}_\nu = \frac{2}{Nm_\nu} \sum_{i_\nu=1}^{N/2} \mathbf{p}_{i_\nu},$$

where $\nu = +, -$ denotes positive and negative ions, m_ν is the mass of the ion of type ν, and the index i_ν goes over ions of type ν only. It is assumed that there are equal numbers of ions of each type, and that $\mathbf{u}_\nu$ is entirely in the x direction. From the equipartition theorem, the kinetic temperature is given by

$$\frac{3}{2}Nk_{\mathrm{B}}T_{\mathrm{KIN}} = \sum_{\nu=+,-} \frac{1}{2m_\nu} \left\langle \sum_{i_\nu=1}^{N} (\mathbf{p}_{i_\nu} - m_\nu \mathbf{u}_\nu)^2 \right\rangle. \tag{7}$$

The equations of motion are

$$\begin{aligned} \dot{\mathbf{r}}_i &= \mathbf{p}_i/m_i \\ \dot{\mathbf{p}}_i &= \mathbf{F}_i + \mathbf{i} z_i e E_{\mathrm{EL}} - \alpha \mathbf{p}_i, \end{aligned} \tag{8}$$

where the expression for the thermostat multiplier α is given in Ref. 13.

The "configurational" thermostat is introduced in the same way as in Eq. (6),

$$\begin{aligned} \dot{\mathbf{r}}_i &= \frac{\mathbf{p}_i}{m_i} + \frac{s}{T_0}\frac{\partial T_{\mathrm{CONF}}}{\partial \mathbf{r}_i} \\ \dot{\mathbf{p}}_i &= \mathbf{F}_i + \mathbf{i} z_i e E_{\mathrm{EL}} \\ \dot{s} &= -Q(\mathbf{T}_{\mathrm{CONF}} - \mathbf{T}_0)/\mathbf{T}_0. \end{aligned} \tag{9}$$

Because $\nabla \cdot \nabla(1/r) = 0$, electrostatic interactions do not contribute directly either to the thermostat terms in Eqs. (6) and (9) or to the denominator of Eq. (5).

Simulations were performed on a system consisting of 512 ions (256 ions of each type). In shear flow and alternating electric field simulations, the system was at a density of $\rho = 1500\,\mathrm{kg \cdot m^{-3}}$ and at a temperature of $T = 1500\,\mathrm{K}$, in the middle of the liquid region of the phase diagram [14]. In a constant electric field, simulations were done at the additional supercritical state, at a density of $\rho = 200\,\mathrm{kg \cdot m^{-3}}$ and at a temperature of $T = 3200\,\mathrm{K}$, in order to estimate the effect of density on thermostatting.

The equations of motion were solved using the 5th order Gear predictor–corrector scheme. For the calculation of thermostatted steady-state averages, the system was first equilibrated for 0.5 ns, then brought to the steady state with the field and the appropriate thermostat, in runs that varied in length from 0.5 ns for the lowest field, to 0.25 ns for the highest field. The averages were collected in production runs that were twice the length of the preparation runs.

Electrostatic interactions were treated using the Ewald summation technique [15] with the conducting boundary at infinity. The non-electrostatic and the real space electrostatic interactions were cut off at half the box length, $L/2$, the reciprocal space wave-vector cut-off was at $k_{\max} = 6(2\pi/L)$ and the convergence acceleration factor was chosen as $\kappa = 1.8\pi/L$. For the sheared system governed by Sllod equations, we used the specific form of the Ewald sum [16] consistent with the Lees–Edwards periodic boundary conditions [17].

3. SHEAR FLOW

In nonequilibrium simulations, the shear viscosity η is obtained directly from the constitutive relationship,

$$\eta = -P_{xy}/\gamma, \tag{10}$$

where P_{xy} is the shear stress.

In the low strain rate regime, the response to shear is linear, i.e., the shear viscosity obtained from Eq. (10) is constant. For moderate shear rates, mode-coupling theory predicts a decrease in viscosity proportional to the square root of strain rate,

$$\lim_{\gamma \to 0} \eta(\gamma) = \eta(0) - b\gamma^{1/2}.$$

This type of dependence has been observed in simple liquids, with two regimes of different values of the proportionality constant b as the shear rate increases [18,19]. The same qualitative behavior is found in molten NaCl for strain rates lower than $8\,\mathrm{ps}^{-1}$ (Fig. 1). The viscosity in the linear region is the same for both types of thermostat. For higher values of the strain rate the square-root dependent shear thinning is observed in both cases, but the viscosities obtained with the configurational thermostat are consistently lower.

We intuitively expect that non-thermostatted degrees of freedom heat up in an external field. Specifically, we expect the configurational

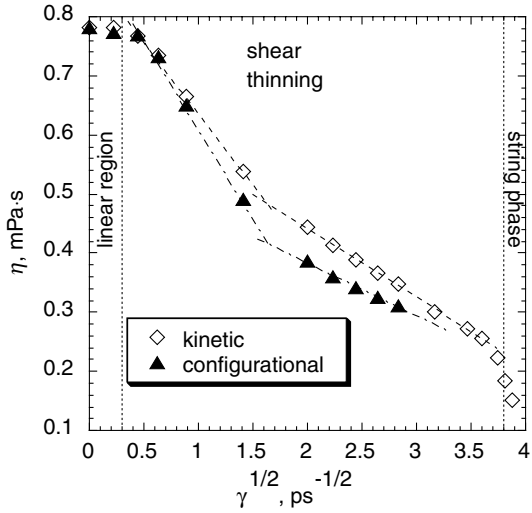

Fig. 1. Shear rate γ dependent viscosity for two thermostats. For low shear rates, the viscosity is constant and the response to shear is linear. For moderate shear rates there are two different shear-thinning regimes where the decrease in viscosity is proportional to $\gamma^{1/2}$. A sharp drop in viscosity accompanied with the appearance of a string phase is found for $\gamma \geqslant 14.5\,\mathrm{ps}^{-1}$ with the kinetic thermostat.

temperature to increase when the kinetic temperature is kept constant, and *vice versa*. Indeed, T_{KIN} increases monotonically in a configurationally thermostatted sheared system. For all sheared systems studied until now, configurational temperature increased with strain rate when a kinetic temperature thermostat was used. For molten NaCl with a kinetic thermostat, however, the configurational temperature with strain rate first decreases, reaches a minimum, and then increases steadily (Fig. 2). If we switch off the electrostatic interactions and simulate "neutral NaCl", we observe the expected monotonic behavior.

In a neutral sheared system with a kinetic thermostat, both the numerator and the denominator of Eq. (5) increase with shear rate, but the numerator increases faster. In the ionic system, the non-monotonic behavior of configurational temperature is the consequence of the non-monotonic dependence of the numerator on shear rate. The sum of squared forces from positive and negative clouds on individual particles increases with strain rate because the pair distribution function is deformed in a sheared system, allowing the particles to come closer to each other. However, the local deviations of positive and negative shells are highly correlated and the forces from positive and negative clouds partially cancel. For low shear rates, this cancellation is a stronger effect

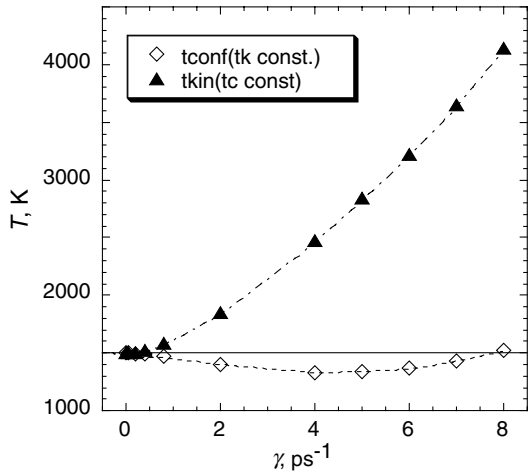

Fig. 2. Shear rate dependence of the configurational temperature in the system with the kinetic thermostat and of the kinetic temperature in the system with the configurational thermostat. The kinetic temperature increases steadily, while the change of the configurational temperature is non-monotonic.

than the increase of mean square forces caused by the closer approach of ions. In this range of shear rates, the correlation between instantaneous local distributions of positive and negative ions is enhanced by the requirement that both types have the same linear streaming velocity profile. This means that the kinetic temperature thermostat artificially changes local structure under shear. For higher shear rates, the increase of mean-square forces dominates. Such correlations cannot occur in a neutral system.

If shear rate is increased even further in a system with the kinetic thermostat, one can observe a sharp drop of viscosity and pressure between $\gamma = 14\,\mathrm{ps}^{-1}$ and $\gamma = 14.5\,\mathrm{ps}^{-1}$. In a projection of all particle positions onto the yz-plane (Fig. 3a), a region of "string phase" appears in coexistence with the liquid phase. It consists of alternating planes of strings of the same charge, parallel to the x-axis and moving in the x direction with different streaming velocities (Fig. 3b). Such string phases appear in strongly sheared neutral systems with kinetic-type thermostats assuming a "linear streaming velocity profile" [4, 20], but have not been observed with the configurational thermostat [4]. Unfortunately, we have not been able to simulate molten NaCl with the configurational thermostat for shear rates stronger than $\gamma = 8\,\mathrm{ps}^{-1}$ because the system of equations became numerically unstable. For example, for $\gamma = 10\,\mathrm{ps}^{-1}$ the system was unstable even for a time step as small as 0.001 fs because of large numerical (integration) errors.

4. CONSTANT ELECTRIC FIELD

4.1. Liquid

In a steady state in an external electric field, oppositely charged ions flow in opposite directions parallel to the field, generating the electric current density,

$$\mathbf{j} = \frac{e}{V} \sum_{i=1}^{N} z_i \mathbf{v}_i . \tag{11}$$

The electric conductivity σ is defined as the ratio of the current density to the field,

$$\boldsymbol{\sigma} = j_x / E_{\mathrm{EL}} . \tag{12}$$

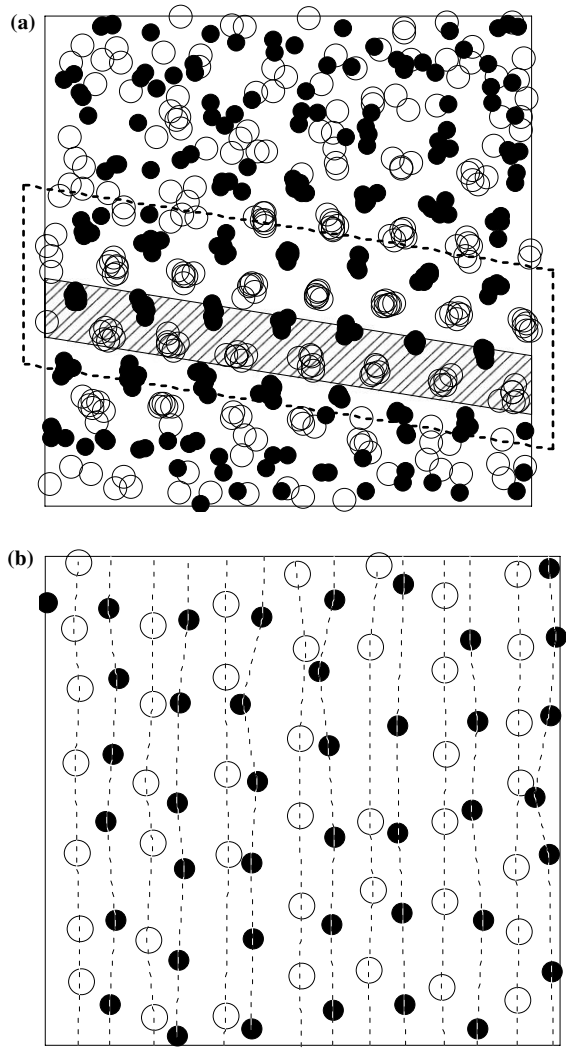

Fig. 3. (a) The projection of all particle positions onto the *yz*-plane. A string phase (in the region surrounded by the dashed line) coexists with a liquid at $\gamma = 15\,\mathrm{ps}^{-1}$. The projection of the shaded layer on the *xy*-plane is shown in (b). The charges of the same sign are organized in strings traveling in the *x*-direction.

The equilibrium conductivity is found from the Green–Kubo integral [10]

$$\sigma = \frac{V}{3k_B T} \int_0^\infty C_{\mathrm{jj}}(t)dt,$$

where C_{jj} is the equilibrium current autocorrelation function,

$$C_{jj}(t) = \langle \mathbf{j}(t) \cdot \mathbf{j}(0) \rangle_{EQ}, \tag{13}$$

Field-dependent conductivities computed with the two thermostats, see Eqs. (8) and (9), are presented in Fig. 4. For fields up to 0.5×10^9 $\mathrm{V{\cdot}m^{-1}}$, conductivities computed with different thermostats agree with the equilibrium result to within the statistical error and the response is linear. After that, flow velocities, currents, and conductivities increase with the field, but agree with each other for fields up to approximately $2.5\times10^9\ \mathrm{V{\cdot}m^{-1}}$. This is the range of fields for which flow velocities $u_\pm$ are small enough compared to average ion velocities obtained from equipartition (Eq. (7)) at this temperature. For higher fields, quantitative differences become noticeable. A smaller response at the same field strength is consistently obtained with the kinetic thermostat (Eq. (8)), while the currents obtained with the configurational thermostat show much faster growth with the field.

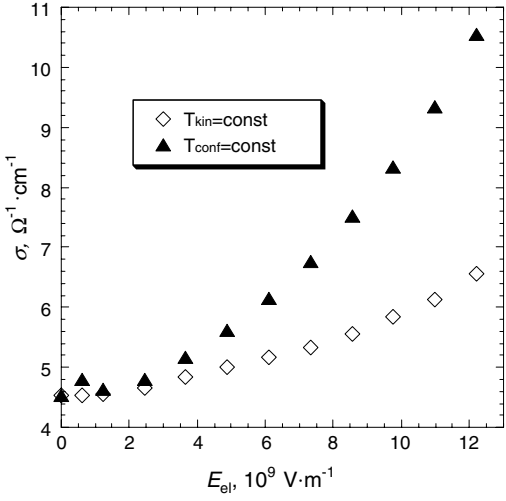

Fig. 4. Electric field dependence of the conductivity for molten NaCl with kinetic and configurational thermostats.

Potential energy grows steadily with the increase in field strength in both cases. The increase in potential energy indicates a shift from the largest part of pair interactions being attractive, to a configuration where repulsive interactions give the largest contribution. The reason for this is in the change of the local structure of the liquid, as described by the pair distribution function g(**r**), in a strong electric field. The pair distribution function g(**r**) ceases to be isotropic. The shells of oppositely charged ions get displaced in the field direction with respect to the central ion, which allows them to approach the central ion closer from one side. At these positions, the non-electrostatic repulsion is much stronger, and the result is the increase in potential energy and pressure. The shell of the ions of the same charge is not displaced, since they move with the same average flow velocity as the central ion. There is only some barely perceptible deformation because of the difference in screening due to the displacement of the oppositely charged shells.

Each of the temperatures increases when the other is constrained. The particularly large increase of kinetic temperature with the configurational thermostat suggests that there exist additional spatially and temporally dependent flows (e.g., longitudinal and transversal traveling waves), which average to zero over the simulation cell, but are part of the response neglected in the kinetic definitions.

4.2. Supercritical Fluid

The equilibrium electric conductivity is an order of magnitude lower than the conductivity in the liquid phase. The reason for this is that the low-density fluid is not fully dissociated, but partly consists of oppositely charged ion pairs and short chains [21], so that only free ions contribute to the current. The responses to the imposed field agree for the two thermostats for a range of fields up to approximately $4.5\times10^9\,\mathrm{V\cdot m^{-1}}$, nearly twice the limit for the liquid (Fig. 5). Even for the lowest field used in simulation ($6.1\times10^8\,\mathrm{V\cdot m^{-1}}$), the response was not linear. Conductivity increases linearly with field, and the values obtained with the two thermostats agree. The potential energy per particle (Fig. 6), pressure and the expression for the unthermostatted temperature (Fig. 7a) slowly increase and match in the two differently thermostatted systems. Qualitative and large quantitative differences appear for fields higher than $5\times10^9\,\mathrm{V\cdot m^{-1}}$. The conductivity for systems with the configurational thermostat starts to dramatically increase with field, while the increase stays more or less linear with the kinetic thermostat. The trends in the behavior of the potential energy per particle and unthermostatted temperature become completely

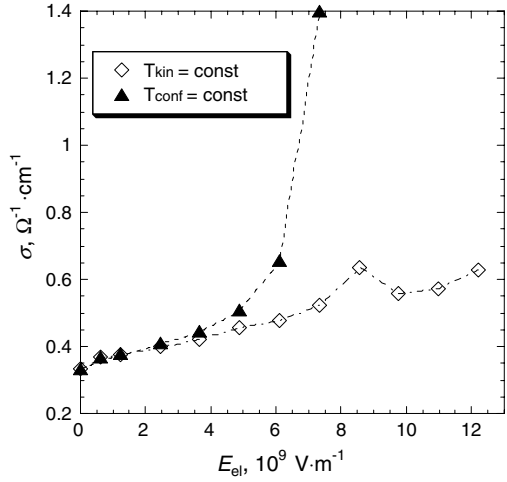

Fig. 5. Electric field dependence of the conductivity of supercritical NaCl with kinetic and configurational thermostats.

opposite. With the configurational thermostat, the potential energy and kinetic temperature increase steeply, whereas with the kinetic thermostat both potential energy and configurational temperature decrease.

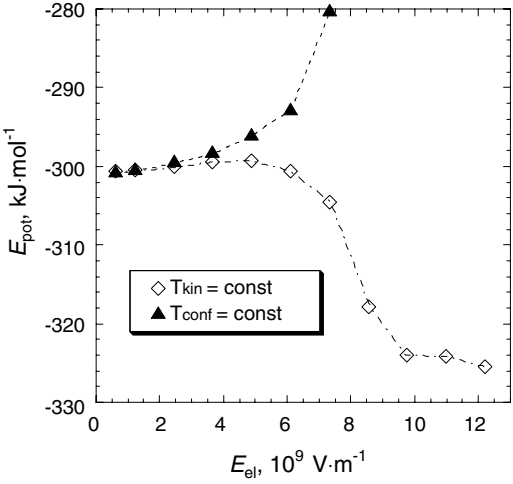

Fig. 6. Electric field dependence of the potential energy per particle for supercritical NaCl with kinetic and configurational thermostats.

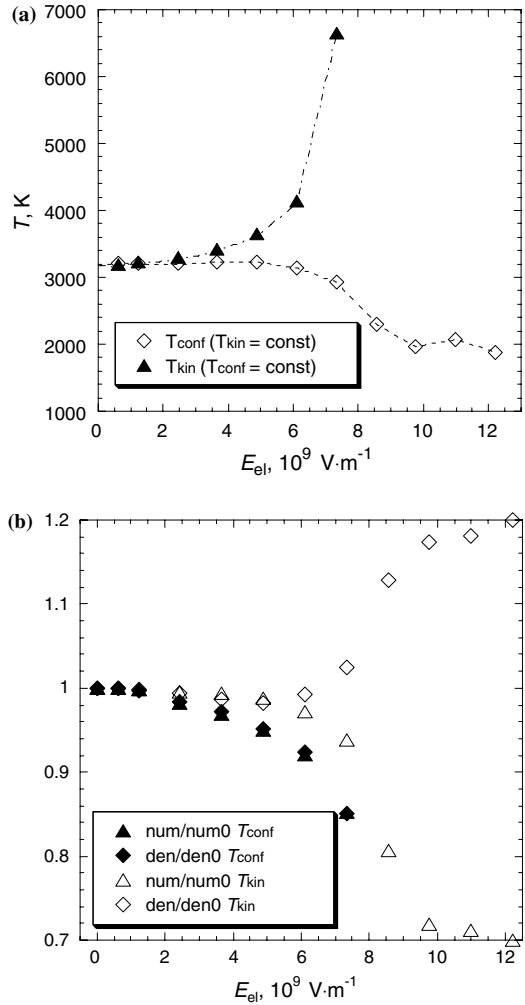

Fig. 7. (a) Electric field dependence of the configurational temperature in the system with the kinetic thermostat and of the kinetic temperature in the system with the configurational thermostat, for liquid NaCl, (b) change of the numerator and of the denominator of the configurational temperature expression (Eq. (5)) with electric field observed for kinetic and configurational thermostats.

These trends can be explained in terms of structure enforced by the specific thermostat. For low fields, the slow increase of the conductivity with field strength is caused by an increased acceleration of an unchanged number of free ions. The field allows them to approach each other more closely before backscattering compared to a system without field, increasing their average potential energy.

At high field strengths, the specific mechanism for extracting excess heat becomes more important. The effect of the kinetic thermostat is equivalent to continuous rescaling of velocities in order to keep the kinetic energy constant relative to flow. As oppositely charged ions accelerate towards each other, their potential energy falls, and their kinetic energy would grow in a constant energy simulation. This acceleration is interpreted as heating and is suppressed by the thermostat, decreasing the total energy of the accelerating ion. As a consequence, it becomes more probable for an ion to get caught in the potential well of an oppositely charged ion and form an associated pair. Therefore, the thermostat of the type given by Eq. (8) enhances the probability of association and somewhat decreases the number of free ions contributing to the current as the field increases, while the remaining free ions move with larger velocity due to the increased field strength. The result of these two trends is that the conductivity increases at a nearly constant rate, while the increased association causes the average potential energy per molecule to decrease.

At high fields the picture is drastically different with the configurational thermostat (Eq. (9)). The rate of increase of current with field is faster than linear, and much faster than in the liquid. The reason is that the kinetic energy is not directly limited. This allows the ion pairs to dissociate, and the increase in current is the result both of acceleration and the increased number of free ions. As they move faster, they can come closer before recoil, and there are also more particles in the attractive tail of the potential energy. This causes the monotonic increase of the average potential energy (Fig. 6) with the field.

While the kinetic temperature increases in a system with a configurational thermostat in accordance with our intuitive expectations, the configurational temperature decreases steadily with the field when the kinetic thermostat (Eq. (8)) is used (Fig. 7a). With an electric field and a kinetic thermostat, the numerator of Eq. (5) decreases, while the denominator increases with field (Fig. 7b). A lower level of dissociation of salt vapor can explain both effects. The potential energy (Eq. (1)) of associated pairs is close to a minimum, where the forces nearly vanish. Associated pairs are neutral (although with a dipole moment) and do not attract shells of alternating charge that are shifted in the field. All this contributes to the decrease of the numerator. The highest contribution to the denominator

is from the pairs with potential energies close to the minimum, so that greater association also causes it to increase.

When the configurational thermostat is used, both the numerator and the denominator decrease at the same rate with the field (Fig. 7(b)). This is different from any other nonequilibrium system investigated so far, where both the numerator and the denominator increased with the field. The decrease in the average force and the denominator is the result of more and more free ions being in the attractive tails of the interaction potential where the forces and their divergences are smaller.

5. ALTERNATING ELECTRIC FIELD

When an alternating electric field of sufficiently small amplitude is applied in the x-direction, the time-dependent current density is given by the linear response formula [10],

$$\langle j_x(t)\rangle = \frac{V}{k_B T}\int_0^t ds \boldsymbol{C}_{jj}(s)\boldsymbol{E}_{\mathrm{EL}}(t-s), \tag{14}$$

or in the Fourier transformed form,

$$\left\langle \tilde{j}_x(\omega)\right\rangle = \tilde{\sigma}(\omega)\tilde{E}_{\mathrm{EL}}(\omega), \tag{15}$$

where $\left\langle \tilde{j}_x(\omega)\right\rangle$ and $\tilde{E}_{\mathrm{EL}}(\omega)$ are the Fourier transforms of the ensemble-averaged current and field, and $\tilde{\sigma}(\omega)$ is the complex spectral density of the current autocorrelation function,

$$\tilde{\sigma}(\omega) = \int_0^\infty dt e^{i\omega t} C_{jj}(t). \tag{16}$$

The time dependent response to a "monochromatic" electric field $E_{\mathrm{EL}} = E_0 \cos\omega_0 t$ in a "final periodic state" when the transients have decayed, has the form

$$\langle j_x(t)\rangle = \mathrm{Re}\left[\tilde{\sigma}(\omega_0)\right] E_0 \cos\omega_0 t - \mathrm{Im}\left[\tilde{\sigma}(\omega_0)\right] E_0 \sin\omega_0 t. \tag{17}$$

The in-phase part of the response is determined by the real part of the spectral density, and the out-of-phase part is determined by its imaginary part.

The equilibrium spectral density $\tilde{\sigma}(\omega)$ at the liquid state point is shown in Fig. 8. The amplitude $|\tilde{\sigma}(\omega)|$ shows a resonance peak for $\omega/2\pi \approx$

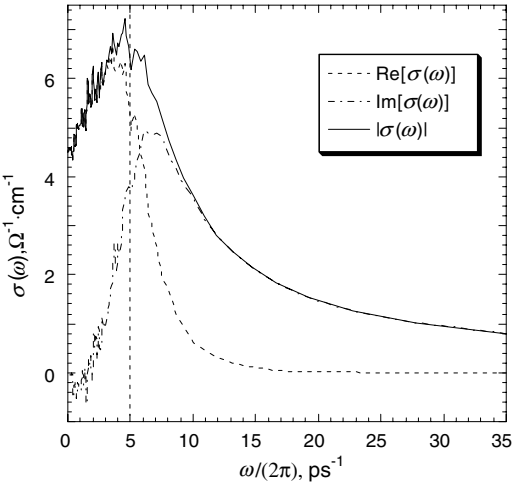

Fig. 8. Spectral density of the equilibrium current autocorrelation function.

$5\,\mathrm{ps}^{-1}$, which is approximately the characteristic frequency obtained from the Taylor expansion of the positive–negative ion pair potential energy (Eq. (1)) around the bottom of the potential well. This is the frequency ω_P of the "plasmon mode" present in the tail of the current autocorrelation function. The negative values of the imaginary part obtained for very low frequencies are a consequence of the negative long-time tail of the autocorrelation function.

In the linear response region of E_0 and ω, the amplitude of $\left\langle \tilde{j}_x(\omega) \right\rangle / E_0$ is equal to $|\tilde{\sigma}(\omega)|$, and the phase lag ϕ of the current behind the field is determined from

$$\tan\phi = -\mathrm{Im}\,[\tilde{\sigma}(\omega)]/\mathrm{Re}\,[\tilde{\sigma}(\omega)].$$

In Fig. 9 we compare the responses $\left\langle \tilde{j}_x(\omega) \right\rangle / E_0$ to the equilibrium spectral density for electric fields of two amplitudes of 4.8×10^9 and $12.2\times10^9\,\mathrm{V\cdot m}^{-1}$ for a range of frequencies.

For high frequencies ($\omega/2\pi \geqslant 10\,\mathrm{ps}^{-1}$) the response is linear for both field amplitudes. For $E_0 = 4.8\times10^9\,\mathrm{V\cdot m}^{-1}$ with the kinetic thermostat, it is linear for all investigated frequencies except $\omega = 0$, while with the configurational thermostat small non-linearities appear for $\omega/2\pi \leqslant 5\,\mathrm{ps}^{-1}$. As the frequency decreases below this value, the amplitude decreases, reaches a minimum and then increases towards the steady-state value of the conductivity for this field. For $E_0 = 12.2\times10^9\,\mathrm{V\cdot m}^{-1}$ the differences between the responses with the two thermostats at low frequencies are much more

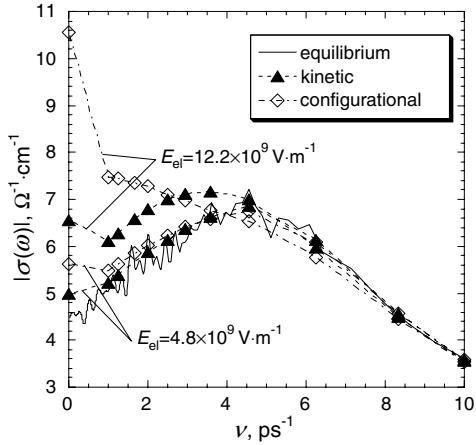

Fig. 9. Frequency-dependent conductivity and phase lag for two electric field amplitudes.

prominent and start to show already for $\omega/2\pi \geqslant 10\,\mathrm{ps}^{-1}$. With the kinetic thermostat, there is a shift towards lower resonance frequency associated with increased damping, and a more pronounced minimum of amplitude between resonance and zero frequency. With the configurational thermostat, the resonance disappears altogether and the frequency dependence of the amplitude has an overdamped appearance. Nevertheless, for very low frequencies the amplitude is larger than with the kinetic thermostat. For the lowest investigated frequency of $0.5\,\mathrm{ps}^{-1}$ the amplitude did not seem to converge to the constant field value. Since the shape of $\langle j_x(t)\rangle$ during one period is quite distorted by the presence of the higher harmonics, it is possible that there is a discontinuity in the amplitude at very low frequencies, characteristic of nonlinear oscillations. This effect is currently under investigation.

6. CONCLUSIONS

We have investigated the behavior of molten sodium chloride subjected to strong shear and strong constant or alternating electric fields, and the dependence of the simulation results on the type of thermostatting method. We found that the response is linear for a huge range of shear rates (up to $\sim 0.05\,\mathrm{ps}^{-1}$) and constant electric field magnitudes (up to $\sim 0.5 \times 10^9\,\mathrm{V{\cdot}m}^{-1}$). In alternating electric fields, the response is linear for larger amplitudes if the frequency is higher. As long as the response is linear, simulation results do not depend on the type of thermostat. In this case one may choose to use the kinetic thermostat due to its simplicity and efficiency.

In the nonlinear region there are differences in the response depending on the type of thermostat used in simulations. The configurational temperature approach is then preferred because of the uncertainty of the flow profile in the kinetic control schemes.

Sheared molten NaCl exhibits shear thinning, much like a simple liquid. The difference in viscosities with different thermostats is only quantitative; the values obtained with the configurational thermostat are lower than with the kinetic thermostat. The situation is similar in an electric field, with the electric conductivity increasing faster with field if the configurational thermostat is used.

Qualitative differences appear only for extremely strong perturbations. Under extreme shear, a string phase is formed with the kinetic thermostat, while with the configurational thermostat the trajectories become very unstable. For a supercritical fluid in an extremely strong constant electric field, the structural differences are even more spectacular. The kinetic thermostat leads to enhanced association, while a configurational thermostat results in an increase in dissociation of ion pairs and chains. For a liquid in alternating fields, the differences can be observed for large field amplitudes and low frequencies. With a configurational thermostat the resonance frequency disappears and there seems to be a discontinuity in the dependence of the amplitude on frequency characteristic of a strongly anharmonic response. In accordance with this, the presence of higher harmonics in the current is much more prominent than with the kinetic thermostat. This suggests that the kinetic thermostat interprets higher harmonics as thermal motion and partially suppresses them.

ACKNOWLEDGMENT

We wish to thank the National Facility of Australian Partnership for Advanced Computing for a substantial allocation of computer time for this project.

REFERENCES

1. D. J. Evans, W. G. Hoover, B. H. Failor, B. Moran, and A. J. C. Ladd, *Phys. Rev*. A **28**:1016 (1983).
2. W. G. Hoover, *Phys. Rev. A* **31**:1695 (1985).
3. D. J. Evans and G. P. Morriss, *Phys. Rev. Lett*. **56**:2172 (1986).
4. J. Delhommelle, J. Petravic, and D. J. Evans, *Phys. Rev. E* **68**:031201/1-6 (2003).
5. H. H. Rugh, *Phys. Rev. Lett*. **78**:772 (1997).
6. O. G. Jepps, G. Ayton, and D. J. Evans, *Phys. Rev. E* **62**:4757 (2000).
7. J. Delhommelle and J. Petravic, *J. Chem. Phys*. **118**:2783 (2003).
8. J. Petravic and J. Delhommelle, *J. Chem. Phys*. **118**:7477 (2003).

9. M. P. Tosi and F. G. Fumi, *J. Phys. Chem. Solids* **25**:31 (1964).
10. D. J. Evans and G. P. Morriss, *Statistical Mechanics of Nonequilibrium Liquids* (Academic Press, London, 1990).
11. L. Lue, O. G. Jepps, J. Delhommelle, and D. J. Evans, *Mol. Phys*. **100**:2331 (2002).
12. S. R. de Groot and P. Mazur, *Non-equilibrium Thermodynamics* (Dover, New York, 1984).
13. D. MacGowan and D. J. Evans, *Phys. Rev. A* **34**:2133 (1986).
14. Y. Guissani and B. Guillot, *J. Chem. Phys*. **101**:490 (1994).
15. S. Nosé and M. L. Klein, *Mol. Phys*. **50**:1055 (1983).
16. D. R. Wheeler and R. L. Rowley, *Mol. Phys*. **94**:555 (1998).
17. A. W. Lees and S. F. Edwards, *J. Phys. Ser. C* **5**:1921 (1972).
18. K. P. Travis, D. J. Searles, and D. J. Evans, *Mol. Phys*. **95**:195 (1998).
19. I. Borzsak, P. T. Cummings, and D. J. Evans, *Mol. Phys*. **100**:2735 (2002).
20. J. J. Erpenbeck, *Phys. Rev. Lett*. **52**:1333 (1984).
21. K. S. Pitzer, *J. Chem. Phys*. **104**:6724 (1996).